

# Aftershocks' Effect on Structural Design Actions in Italy

by Iunio Iervolino, Eugenio Chioccarelli, and Massimiliano Giorgio

**Abstract** Although earthquakes generally form clusters in both space and time, only mainshocks, usually the largest magnitude events within clusters, are considered by probabilistic seismic hazard analysis (PSHA; [Cornell, 1968](#)). On the other hand, aftershock PSHA (APSHA), based on the modified Omori law, allows the quantification of the aftershock threat ([Yeo and Cornell, 2009](#)). Classical PSHA often describes event occurrence via a homogeneous Poisson process, whereas APSHA describes occurrence of aftershocks via cluster-specific nonhomogeneous Poisson processes, the rate of which is a function of the mainshock magnitude. It is easy to recognize that clusters, each of which is made of the mainshock and the following aftershocks, occur at the same rate of mainshocks. This recently allowed the generalization of the hazard integral to account for aftershocks in PSHA (i.e., [Iervolino et al., 2014](#)), which resulted in the formulation of the so-called sequence-based PSHA (SPSHA). In the present study, SPSHA is applied to Italy countrywide, using the same source model ([Stucchi et al., 2011](#)) that lies at the base of the official PSHA used for structural design, to quantitatively assess the increase in seismic design actions for structures when accounting for the aftershocks.

## Introduction

The state of advanced structural engineering codes is such that design seismic accelerations are derived from probabilistic seismic hazard analysis (PSHA; [Cornell, 1968](#); [McGuire, 2004](#)). PSHA provides, for a site of interest, the ground-motion intensity measure (IM) value that corresponds to a given rate of exceedance. The IM is typically an ordinate of a (pseudo) acceleration response spectrum, and structures must be designed against values corresponding to rates that are functions of the desired seismic performance.

Even if seismic events generally occur in time–space clusters, classical PSHA describes the occurrence of earthquakes via a homogeneous Poisson process (HPP). This model is used to determine seismic design actions in Italy (the case investigated herein), however, other occurrence processes can be used for PSHA; see, e.g., [Beauval et al., 2006](#), or [Polidoro et al., 2013](#). From the HPP assumption of earthquake occurrence, it follows that the events causing the exceedance of an IM value at a site of interest occur according to an HPP ([Cornell, 1968](#)). To be compatible with this modeling hypothesis, only mainshocks, typically the largest magnitude earthquakes within clusters, are considered, via procedures generally known as catalog declustering (e.g., [Gardner and Knopoff, 1974](#)).

For short-term risk management purposes during seismic sequences, aftershock PSHA (APSHA) has been developed ([Yeo and Cornell, 2009](#)). APSHA models the occurrence of aftershocks via cluster-specific nonhomogeneous Poisson processes (NHPP), the rate of which is a function

of the magnitude of the mainshock that has triggered the sequence, via the modified Omori law ([Utsu, 1961](#)). Because earthquake sequences, made of mainshocks and following aftershocks, occur at the same rate as the mainshocks, it is possible to combine HPP-based PSHA and APSHA to include the effect of aftershocks in PSHA, still working with a declustered catalog. The mathematics of this stochastic model, named sequence-based PSHA (SPSHA), was presented in [Iervolino et al. \(2014\)](#).

For any given IM value, SPSHA provides the rate of mainshock–aftershock clusters that cause its exceedance at the site, and its main advantages are: (1) it is probabilistically rigorous in the framework of PSHA and APSHA, (2) it allows the retention of the HPP hypothesis for their occurrence, and (3) it avoids the issues of nondeclustered catalogs such as completeness (see also [Marzocchi and Taroni, 2014](#)). It should also be noted that SPSHA, although stimulated by the work of [Boyd \(2012\)](#), is different mainly because it does not consider foreshocks, makes recourse to APSHA to describe aftershocks, and provides an analytical framework extending the classical PSHA integral.

To quantify the effect of aftershocks on design accelerations, SPSHA is applied herein to Italy to develop maps of two spectral (pseudo) accelerations corresponding to four return periods, those that are most common for design of structures according to the Italian seismic code. To this aim, the same source model (i.e., [Meletti et al., 2008](#)) of the current official seismic hazard ([Stucchi et al., 2011](#)) of Italy

is considered. The obtained SPSHA maps are compared with those based on the same source model, yet from classical PSHA, to help in quantitatively assessing the effects of aftershocks for structural design, a relevant issue from the earthquake engineering perspective.

The remainder of the article is structured such that the essentials of SPSHA are recalled first. Then, disaggregation of SPSHA, not originally provided in Iervolino *et al.* (2014), is formulated. It allows the assessment of how much the exceedance of a ground-motion IM value is contributed by aftershocks with respect to mainshocks, and it is helpful for the scope of this study. Subsequently, after introducing the considered source model for Italy, SPSHA results, in terms of countrywide maps of spectral accelerations for given return periods of exceedance, are presented along with the PSHA counterpart. Moreover, two sites, exposed to comparatively low and high hazard according to PSHA, are also considered for more detailed discussions. The modeling consistency between PSHA and SPSHA allows, finally, the direct comparison of the obtained results and the discussion of the engineering significance of accounting for aftershocks in seismic hazard assessment in Italy.

### Sequence-Based Probabilistic Seismic Hazard Analysis

The main result of PSHA for a site of interest is the average number of earthquakes in one year (i.e., the rate) causing exceedance of a given IM threshold, say  $im$ . The rate of exceedance of  $im$ , herein indicated as  $\lambda_{im,E}$ , is typically obtained via the following equation, which is written, for simplicity, for the case of a single seismic source zone:

$$\lambda_{im,E} = \nu_E \cdot \int_{r_{E,\min}}^{r_{E,\max}} \int_{m_{E,\min}}^{m_{E,\max}} P[\text{IM}_E > im | x, y] \cdot f_{M_E, R_E}(x, y) \cdot dx \cdot dy, \quad (1)$$

and in which  $\nu_E$  is the rate, from a declustered catalog (e.g., Reiter, 1990), of earthquakes above a minimum magnitude of interest ( $m_{E,\min}$ ) and below the maximum magnitude ( $m_{E,\max}$ ) of the considered seismic source. The term  $P[\text{IM}_E > im | x, y]$ , provided by a ground-motion prediction equation (GMPE), represents the probability that the intensity threshold is exceeded given an earthquake of magnitude  $M_E = x$ , from which the site is separated by a distance

$$\lambda_{im} = \nu_E \cdot \left\{ 1 - \iint_{M_E, R_E} P[\text{IM}_E \leq im | x, y] \cdot e^{-E[N_{A|x}(0, \Delta T_A)]} \cdot \iint_{M_A, R_A} P[\text{IM}_A > im | w, z] \cdot f_{M_A, R_A | M_E, R_E}(w, z | x, y) \cdot dw \cdot dz \cdot f_{M_E, R_E}(x, y) \cdot dx \cdot dy \right\}, \quad (2)$$

$R_E = y$ , and  $R_E \in (r_{E,\min}, r_{E,\max})$ . The term  $f_{M_E, R_E}$  is the joint probability density function (PDF) of mainshock magnitude and distance random variables (RVs). For each source, these two RVs are usually considered stochastically independent;  $f_{M_E}$  can be, for example, described by a truncated exponen-

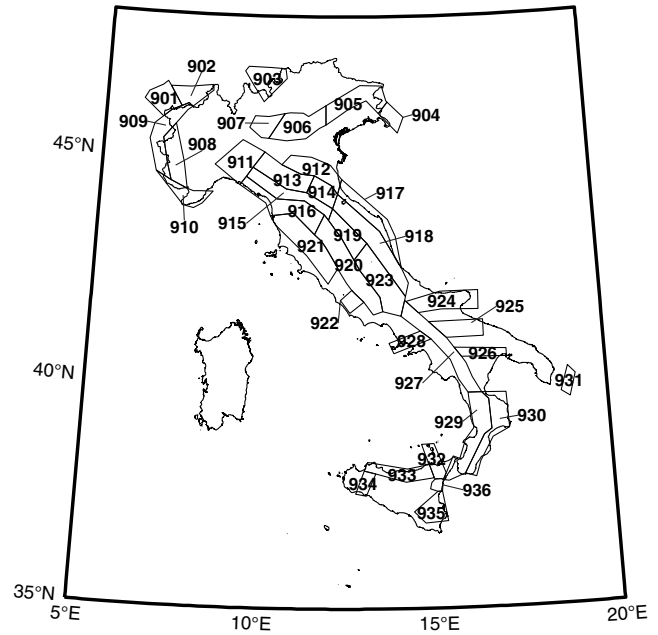


**Figure 1.** The seismic source zone model for Italy, according to the model of Meletti *et al.* (2008).

tial distribution, derived by the Gutenberg–Richter (GR) relationship (Gutenberg and Richter, 1944), and  $f_{R_E}$  is obtained on the basis of the source–site geometrical configuration. The integral limits are the magnitudes bounding the magnitude PDF and the distances defining the domain of possible  $R_E$  values.

Because  $\nu_E$  is from a declustered catalog, and  $f_{M_E, R_E}$  refers to mainshocks, the subscript ( $E$ ) was added to distinguish the obtained rate  $\lambda_{im,E}$  from the one by SPSHA, to follow. Finally, in the case of multiple seismic source, say  $s$  in number, equation (1) is computed one source at a time and the results summed up:  $\lambda_{im,E} = \sum_{i=1}^s \lambda_{im,E,i}$ .

SPSHA aims to evaluate the average number of seismic sequences (mainshocks and following aftershocks) that in one year cause at least one exceedance of  $im$  at the site. This rate is called  $\lambda_{im}$  and is still that of an HPP. It was demonstrated in Iervolino *et al.* (2014) that, under the hypotheses for aftershock hazard of Yeo and Cornell (2009),  $\lambda_{im}$  can be computed via the following equation; that is, a generalization of equation (1):

and in which  $\nu_E$ ,  $P[\text{IM}_E \leq im | x, y] = 1 - P[\text{IM}_E > im | x, y]$ , and  $f_{M_E, R_E}(x, y)$  are the same as defined in equation (1), so also are  $M_E \in (m_{E,\min}, m_{E,\max})$  and  $R_E \in (r_{E,\min}, r_{E,\max})$ , that is, the integral limits are also the same. The exponential term within the integral refers to aftershocks and is worth a

description. It is the probability that none of the aftershocks, following the mainshock of features  $\{M_E = x, R_E = y\}$ , cause exceedance of  $im$ . This probability depends on  $P[IM_A > im|w, z]$ ; that is, the probability that  $im$  is exceeded given an aftershock of magnitude  $M_A = w$  and source-to-site distance  $R_A = z$ . The term  $f_{M_A, R_A|M_E, R_E}$  is the distribution of magnitude and distance of aftershocks, which are conditional on the features  $\{M_E, R_E\}$  of the mainshock. This distribution can be written as  $f_{M_A, R_A|M_E, R_E} = f_{M_A|M_E} \cdot f_{R_A|M_E, R_E}$ , in which  $f_{M_A|M_E}$  is the PDF of aftershock magnitude (i.e., GR type), and  $f_{R_A|M_E, R_E}$  is the distribution of the distance of the site to the aftershocks. The aftershock magnitude is bounded by a minimum magnitude  $m_{\min}$  and the mainshock magnitude; that is,  $M_A \in (m_{\min}, x)$ . ( $m_{\min}$  may coincide with the minimum mainshock magnitude, that is,  $m_{\min} \equiv m_{E, \min}$ .) Given the location of the site, the aftershock distance  $R_A \in (r_{A, \min}, r_{A, \max})$  depends on the magnitude and location of the mainshock (see Iervolino *et al.*, 2014, for details).  $E[N_{A|x}(0, \Delta T_A)]$  is the expected number of aftershocks, due to the mainshock of magnitude  $M_E = x$ , in the  $\Delta T_A$  time interval, which is the considered length of the aftershock sequence (assuming that the mainshock occurred at  $t = 0$ ). This number, consistent with APSHA, can be computed as in the following equation, in which  $\{a, b, c, p\}$  are the parameters of the modified Omori law (Yeo and Cornell, 2009):

$$E[N_{A|x}(0, \Delta T_A)] = \frac{10^{a+b \cdot (x-m_{\min})} - 10^a}{p-1} \cdot [c^{1-p} - (\Delta T_A + c)^{1-p}]. \quad (3)$$

In fact, equation (2) represents a hazard integral for aftershocks (the exponential term) conditional to  $M_E = x$  and  $R_E = y$ , nested in a classical PSHA integral. It is

$$P[IM_E \leq im \cap IM_{UA} > im | IM_E > im \cup IM_{UA} > im] = \frac{\nu_E}{\lambda_{im}} \cdot \iint_{M_E, R_E} P[IM_E \leq im | x, y] \cdot \left( 1 - e^{-E[N_{A|x}(0, \Delta T_A)] \cdot \iint_{M_A, R_A} P[IM_A > im | w, z] \cdot f_{M_A, R_A|M_E, R_E}(w, z | x, y) \cdot dw \cdot dz} \right) \cdot f_{M_E, R_E}(x, y) \cdot dx \cdot dy. \quad (4)$$

easy to recognize that it must be  $\lambda_{im} \geq \lambda_{im, E}$ ; that is, accounting for aftershocks necessarily increases the hazard. Moreover, equation (2) precisely degenerates in equation (1) in case aftershocks are neglected; that is,  $E[N_{A|x}(0, \Delta T_A)] = 0 \quad \forall x \in (m_{E, \min}, m_{E, \max})$ . Thus, the latter equation generalizes the former.

Finally, it should be noted that, for design, earthquake engineering is interested in the probability that at least one exceedance of the ground-motion intensity threshold is observed during the design life of the structure  $\Delta T$ . In SPSHA,

because the computed rate is still that of an HPP, such a probability can be computed via  $1 - e^{-\lambda_{im} \cdot \Delta t}$ , exactly as in the PSHA case. Thus, design seismic actions can be updated to account for the aftershock effect within the classical probabilistic framework.

#### Aftershock Disaggregation

A side result of SPSHA formulation is the probability that exceedance of  $im$  is caused by an aftershock rather than by a mainshock. This probability, which quantifies the contribution of aftershocks to hazard, can be regarded as a disaggregation in much the same way classical hazard disaggregation (e.g., Iervolino *et al.*, 2011) provides the probability that exceedance of design accelerations is caused by specific magnitude–distance pairs, or other RVs possibly involved in the hazard assessment.

SPSHA disaggregation is defined in equation (4) as  $P[IM_E \leq im \cap IM_{UA} > im | IM_E > im \cup IM_{UA} > im]$ . The symbol  $IM_E$  represents the mainshock IM, whereas  $IM_{UA}$  is the maximum IM of the following aftershock sequence. Given that exceedance of  $im$  has been observed during the mainshock–aftershock sequence due to the mainshock or at least one of the aftershocks, that is ( $IM_E > im \cup IM_{UA} > im$ ), the sought probability is the

conditional probability that it was in fact an aftershock that caused the exceedance, while the mainshock was below the threshold; that is, ( $IM_{UA} > im \cap IM_E \leq im$ ),

The equation, the derivation of which is given in the Appendix, uses terms already introduced to define SPSHA. It will be useful for the scope of this work, as illustrated in the following countrywide application to Italy.

#### SPSHA for Italy

##### Mainshock Model (Classical Hazard)

The source model considered herein for Italy is the one by Meletti *et al.* (2008), which features 36 seismic source

zones (Fig. 1) and lies at the core of the Italian hazard study described in [Stucchi \*et al.\* \(2011\)](#). The latter, in turn, provides uniform hazard spectra (UHS) to define engineering structural seismic actions according to the enforced code.

The seismic hazard study of [Stucchi \*et al.\* \(2011\)](#) features a fairly complex logic tree. Herein, the branch named 921 is considered; it is the single branch producing the hazard results that are considered to be the closest to those of the full logic tree (this is for simplicity only, as modeling uncertainty can be considered in SPSHA in analogy to what was done in PSHA). The branch 921 (not to be confused with one of the seismic source zones) considers the mentioned zones and the GMPE by [Ambraseys \*et al.\* \(1996\)](#) to compute  $P[IM_E > im|x, y]$  on rock soil conditions.

Herein, the GMPE is applied within its definition ranges of magnitude and distance: these are magnitudes between 4.0 and 7.5 and the closest horizontal distance to the surface projection of the fault plane up to 200 km. The effects of earthquakes with magnitude or distance outside these intervals are neglected. Assuming a uniform epicenter distribution in each seismogenic zone, epicentral distance is converted into the metric required by the GMPE according to [Montaldo \*et al.\* \(2005\)](#). The style-of-faulting correction factors proposed by [Bommer \*et al.\* \(2003\)](#) are also applied to the GMPE, consistent with the rupture mechanism associated with each seismic source zone by [Meletti \*et al.\* \(2008\)](#).

The mainshock rates of the zones in branch 921 of [Stucchi \*et al.\* \(2011\)](#) are not provided as GR relationships, but for surface-wave magnitude bins. These, provided by Carlo Meletti (see [Data and Resources](#)), are given in Table 1. The central magnitude of the lowest bin is generally 4.3 (apart from the zone 936 that is the Etna's volcanic area and has a central magnitude of the lower bin equal to 3.7), whereas the maximum depends on the zone of interest (it can be inferred from the largest magnitude bin with rate larger than zero in Table 1).

This model is used to compute PSHA for the country (to provide a point of comparison), as well as to compute SPSHA, which considers the same mainshock rates and zones.

#### Aftershock Model

The parameters used in the modified Omori law, equation (3), are from [Lolli and Gasperini \(2003\)](#) for generic Italian aftershock sequences:  $a = -1.66$ ,  $b = 0.96$ ,  $c = 0.03$  (in days), and  $p = 0.93$ . The minimum magnitude of generated aftershocks ( $m_{\min}$ ) corresponds to the minimum mainshock magnitude of the seismic source zones: that is, 4.15 for all the seismogenic zones except zone 936, where it is 4.0. Indeed, zone 936 is able to generate earthquakes with magnitude lower than 4.0; however, the GMPE is applied within its definition range, which constrains the aftershocks' minimum magnitude to 4.0.

It is assumed that aftershocks are located, with uniform probability, in a circular area centered on the mainshock location. The size of this area  $S_A$  depends on the magnitude

of the mainshock ( $M_E = x$ ) via the following equation, in squared kilometers ([Utsu, 1970](#)):

$$S_A = 10^{x-4.1}. \quad (5)$$

#### Working Hypotheses

Some working hypotheses that were taken mostly for simplicity are not believed to affect the general conclusions; nevertheless, they could possibly be refined in more detailed studies.

The aftershock area is considered circular for simplicity, although an elliptical shape, oriented as the Apennines mountain chain (in central Italy), which is the typical strike orientation in the region, would better reflect knowledge of seismicity. Within the aftershock area, locations are uniformly distributed, while their probability is zero outside. On the other hand, an aftershock probability gradually decreasing as the distance from the mainshock increases is often preferred (it was verified in [Iervolino \*et al.\*, 2014](#) that this hypothesis negligibly affects the results). Moreover, the limits of the aftershock area can exceed the boundaries of the seismic source zone.

Equation (5) was originally calibrated for  $5.5 < M_E < 7.5$ ; in the applications shown in this article, it is extended to the minimum magnitudes considered. The [Ambraseys \*et al.\* \(1996\)](#) GMPE is used for both  $P[IM_A > im|w, z]$  and  $P[IM_E \leq im|x, y]$  terms of equation (2); that is, for both mainshock and aftershocks, also keeping the same style of faulting recommended for the zone in question by [Meletti \*et al.\* \(2008\)](#).

Finally, following [Yeo and Cornell \(2009\)](#), the duration of the aftershock sequence ( $\Delta T_A$ ) was considered arbitrarily equal to 90 days from the occurrence of the mainshock, although, in principle, this duration could be mainshock magnitude dependent. In any case, it has been verified that assuming  $\Delta T_A = 365$  days leads to minor differences in results compared with  $\Delta T_A = 90$  days.

#### Analysis and Results

In the following sections, SPSHA results for Italy are presented along with their PSHA counterparts (all calculations are carried out via a recent version of the software described in [Iervolino \*et al.\*, 2016](#)). First, hazard maps are reported for several return periods and two spectral ordinates. Then, considering two specific sites, hazard curves, UHS, and aftershock disaggregation are provided and discussed.

#### Hazard Maps

To compute hazard maps, a uniformly spaced grid of more than 4000 points covering the inland Italian territory is considered. Peak ground acceleration (PGA) and spectral accelerations at 1 s natural vibration period  $SA(1\text{ s})$  on rock are considered as the IMs. The hazard maps refer to four return periods ( $T_r$ ): 50, 475, 975, and 2475 yrs. Results are reported in Figures 2 and 3, for PGA and  $SA(1\text{ s})$ , respectively. In each figure, the upper line of panels, that is, maps from (a) to (d),

Table 1  
Annual Rates of Mainshocks for the Seismic Source Model of Figure 1

	Magnitude												
	3.55–3.85	3.85–4.15	4.15–4.45	4.45–4.75	4.75–5.05	5.05–5.35	5.35–5.65	5.65–5.95	5.95–6.25	6.25–6.55	6.55–6.85	6.85–7.15	7.15–7.45
901	0	0	0.0153	0.0076	0.0166	0.0033	0.0021	0.0021	0	0	0	0	0
902	0	0	0.0534	0.0153	0.0166	0.0099	0	0.0064	0.0014	0	0	0	0
903	0	0	0.0992	0.0076	0.0099	0	0	0.0021	0	0	0	0	0
904	0	0	0.0305	0.0153	0	0	0.0042	0	0	0	0	0	0
905	0	0	0.1687	0.0904	0.0254	0.0106	0.0085	0.0071	0	0.0033	0.0022	0	0
906	0	0	0.0663	0.0482	0.0127	0.0021	0.0042	0	0	0.0011	0	0	0
907	0	0	0.0302	0.0301	0.0021	0	0.0021	0.0014	0	0	0	0	0
908	0	0	0.1069	0.0076	0.0166	0.0066	0.0021	0	0	0	0	0	0
909	0	0	0.0305	0.0076	0.0099	0.0066	0.0021	0	0	0	0	0	0
910	0	0	0.0611	0.0076	0	0.0066	0.0021	0.0064	0	0.0014	0	0	0
911	0	0	0.0305	0.0076	0.0099	0	0.0021	0	0	0	0	0	0
912	0	0	0.0482	0.0120	0.0106	0.0148	0.0021	0.0028	0.0012	0	0	0	0
913	0	0	0.1145	0.0602	0.0169	0.0042	0.0085	0.0014	0	0	0	0	0
914	0	0	0.0843	0.0663	0.0148	0.0085	0.0021	0.0057	0.0014	0	0	0	0
915	0	0	0.1832	0.0763	0.0398	0	0.0042	0.0042	0.0014	0.0014	0	0	0
916	0	0	0.0458	0.0305	0.0085	0.0042	0.0021	0	0	0	0	0	0
917	0	0	0.0542	0.0301	0.0114	0.0085	0.0106	0.0064	0.0012	0	0	0	0
918	0	0	0.1527	0.0229	0.0170	0.0057	0.0085	0.0064	0.0042	0.0014	0	0	0
919	0	0	0.1298	0.0534	0.0297	0.0106	0.0042	0.0071	0.0043	0.0025	0	0	0
920	0	0	0.1832	0.0687	0.0568	0.0085	0	0	0	0	0	0	0
921	0	0	0.1756	0.0840	0.0254	0.0085	0.0021	0.0028	0	0	0	0	0
922	0	0	0.0458	0.0229	0.0169	0.0042	0	0	0	0	0	0	0
923	0	0	0.4122	0.0992	0.0767	0.0227	0.0085	0.0106	0.0021	0.0057	0.0043	0.0014	0.0014
924	0	0	0.0687	0.0382	0.0372	0.0279	0.0140	0	0.0042	0	0.0017	0	0
925	0	0	0.0458	0.0153	0.0047	0	0	0	0	0.0033	0.0017	0	0
926	0	0	0.0305	0.0076	0.0186	0	0.0047	0	0	0	0	0	0
927	0	0	0.2150	0.0561	0.0512	0.0093	0.0047	0.0064	0.0021	0.0042	0.0066	0.0066	0
928	0	0	0.0154	0.0153	0.0186	0	0.0042	0.0021	0	0	0	0	0
929	0	0	0.2243	0.0374	0.0651	0.0186	0.0140	0.0140	0.0085	0.0021	0.0017	0.0066	0.0017
930	0	0	0.1028	0.0093	0.0047	0.0093	0.0093	0.0047	0.0021	0.0021	0.0017	0	0
931	0	0	0.0193	0.0192	0	0	0.0047	0	0	0	0	0.0021	0
932	0	0	0.0748	0.0187	0.0166	0.0033	0	0	0.0042	0	0	0	0
933	0	0	0.1145	0.0153	0.0132	0.0199	0.0066	0.0021	0.0021	0	0	0	0
934	0	0	0.0280	0.0001	0.0099	0.0033	0	0	0.0021	0	0	0	0
935	0	0	0.0534	0.0001	0.0166	0.0099	0.0042	0	0.0021	0	0.0023	0	0.0012
936	0.3359	0.0458	0.0382	0.0153	0.0132	0.0033	0	0	0	0	0	0	0

results from PSHA. The lower line, maps from (e) to (h), is the corresponding result from SPSHA. To compare PSHA and SPSHA for the same return period in both figures, one should consider panels (a) and (e) for  $T_r = 50$  yrs, (b) and (f) for  $T_r = 475$  yrs, (c) and (g) for  $T_r = 975$  yrs, and (d) and (h) for  $T_r = 2475$  yrs. It can be preliminarily observed that, in general, the effect of aftershocks tends to be more relevant in areas exposed to comparatively high hazard according to classical PSHA; that is, areas with larger acceleration values in the top panels of Figures 2 and 3.

To more quantitatively assess the hazard increase due to aftershocks, Figure 4 shows absolute differences between SPSHA and PSHA in terms of IMs that, at the same site, correspond to the same return period (e.g., panel [a] of Fig. 4 is the map obtained subtracting the map in panel [a] from that of panel [e] in Fig. 2). Figure 5 reports the percentage increase; that is, it is obtained by dividing the maps in Figure 4 by the corresponding PSHA maps of Figures 2 and 3. It can be observed that (1) absolute differences are

generally larger for larger return periods; (2) considering the same return period, differences in terms of PGA are larger than those in terms of SA(1 s); (3) considering the same return period and the same IM, largest differences are recorded at the sites with the highest maximum magnitude, zones 923, 927, 929, and 935; (4) percentage increases are not monotonic as a function of  $T_r$ ; and (5) percentage increases in terms of PGA are generally larger than those in terms of SA(1 s).

Table 2 summarizes average and maximum percentage differences over the country, and maximum absolute differences from the maps of Figures 4 and 5. Average percentage increases for SA(1 s), as a function of the return period, are between 10.4% and 7%, with the largest value occurring at  $T_r = 50$  yrs. The range for PGA is also around 10%, yet narrower. The maximum percentage increases are about 28% for PGA at  $T_r = 2475$  yrs and 17% for SA(1 s) at  $T_r = 475$  yrs. The former occurs just outside zone 935, and the latter occurs within it. It is interesting to note that, for SA(1 s), the maximum increase does not correspond to

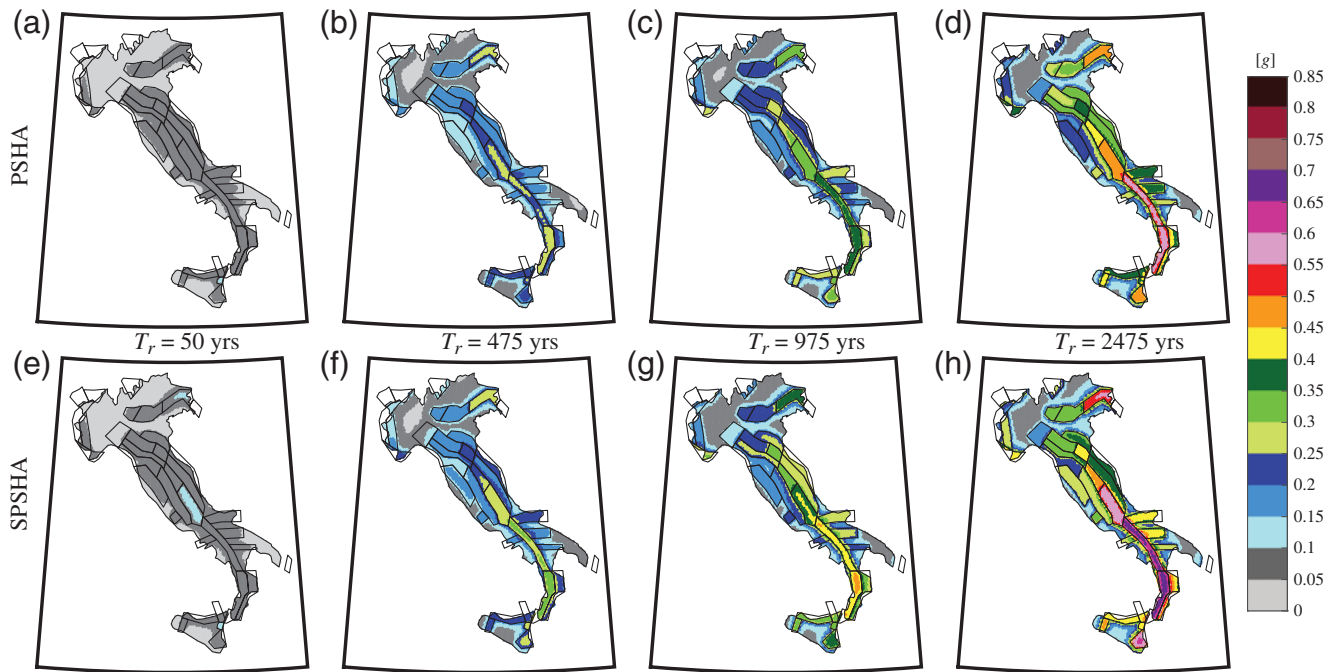


**Figure 2.** Maps of peak ground acceleration (PGA): *im* on rock with four return periods of exceedance equal to 50, 475, 975, and 2475 yrs. (a–d) Are computed via probabilistic seismic hazard analysis (PSHA), and (e–h) are computed via sequence-based PSHA (SPSHA).

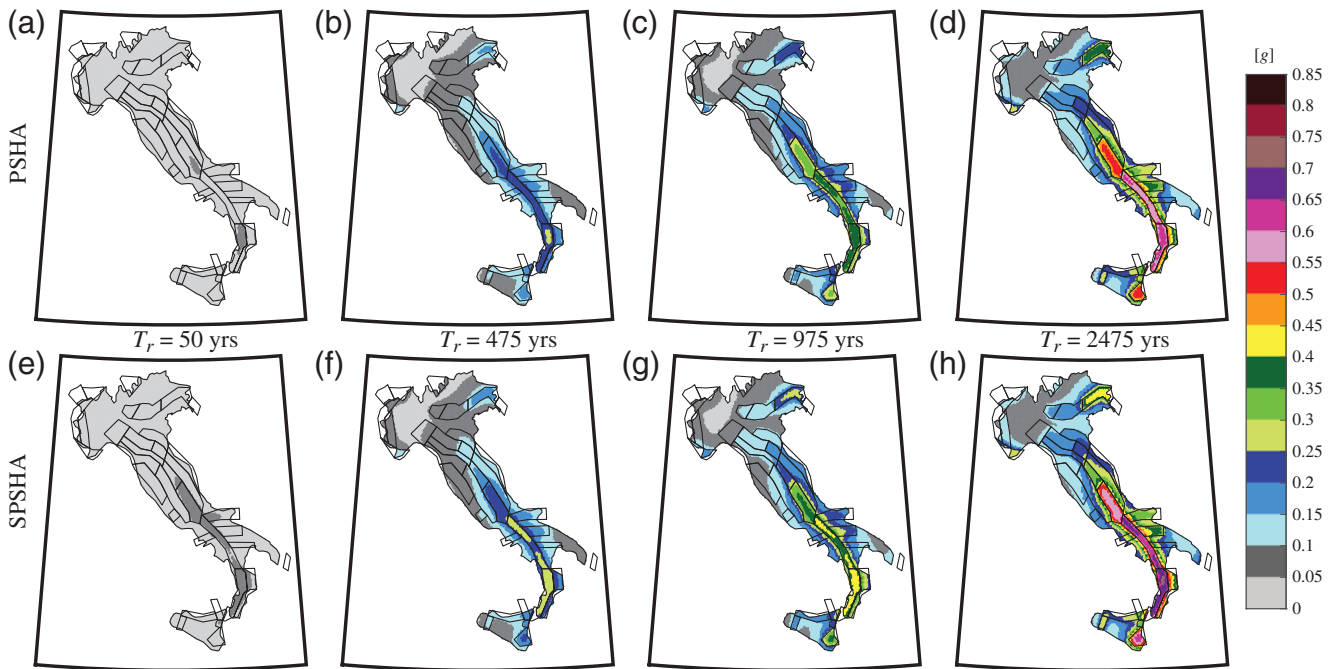


**Figure 3.** Maps of SA(1 s): *im* on rock with four return periods of exceedance equal to 50, 475, 975, and 2475 yrs. (a–d) Are computed via PSHA, and (e–h) are computed via SPSHA.

the largest return period. This issue is explored more deeply in the following sections, in which two specific sites are considered and site-specific hazard curves, UHS, and aftershock disaggregation are reported and discussed. Maximum absolute differences for PGA are equal to 0.012g, 0.058g, 0.084g,

and 0.116g for return periods equal to 50, 475, 975, and 2475 yrs, respectively. The maximum differences in terms of SA(1 s) are equal to 0.007g, 0.035g, 0.051g, and 0.075g for return periods equal to 50, 475, 975, and 2475 yrs, respectively. For PGA, the maximum differences

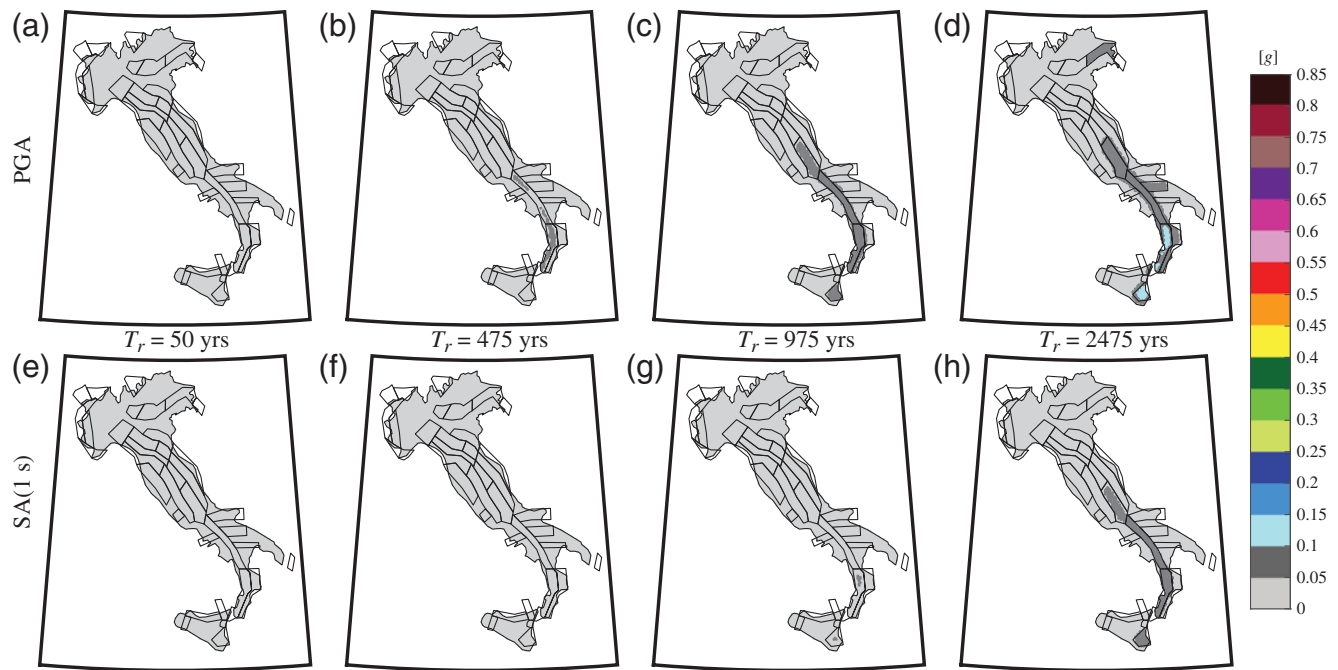


**Figure 4.** Differences between SPSHA and PSHA in terms of *im* with 50, 475, 975, and 2475 yrs return periods of exceedance on rock. (a–d) Refer to PGA, and (e–h) refer to SA(1 s).

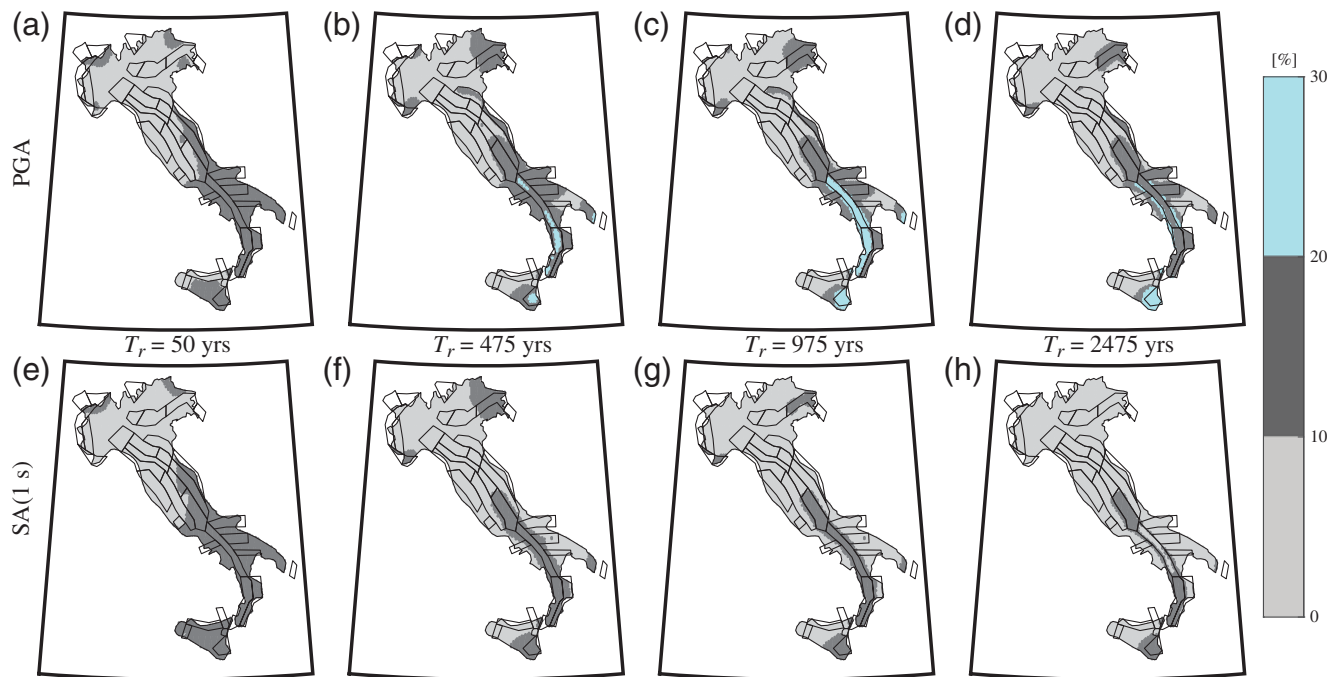


**Figure 5.** Percentage increase from SPSHA with respect to PSHA in terms of *im* with 50, 475, 975, and 2475 yrs return periods of exceedance on rock. (a–d) Refer to PGA; (e–h) refer to SA(1 s).

for return periods up to 975 yrs correspond to sites in zone 929, while the maximum difference for  $T_r = 2475$  yrs occurs at a site enclosed into zone 935; for SA(1 s), the maximum differences for  $T_r = 50$  and 475 yrs occur within zone 929, while they occur within the 935 zone for  $T_r = 975$  and 2475 yrs (see Fig. 1).

#### Site-Specific Hazard Analysis and Aftershocks Disaggregation

Two sites were selected to analyze in more detail the aftershocks' effect on the hazard assessment. The sites are L'Aquila in central Italy (13.40° E, 42.35° N) and Milan in northern Italy (9.18° E, 45.47° N); they are selected to be

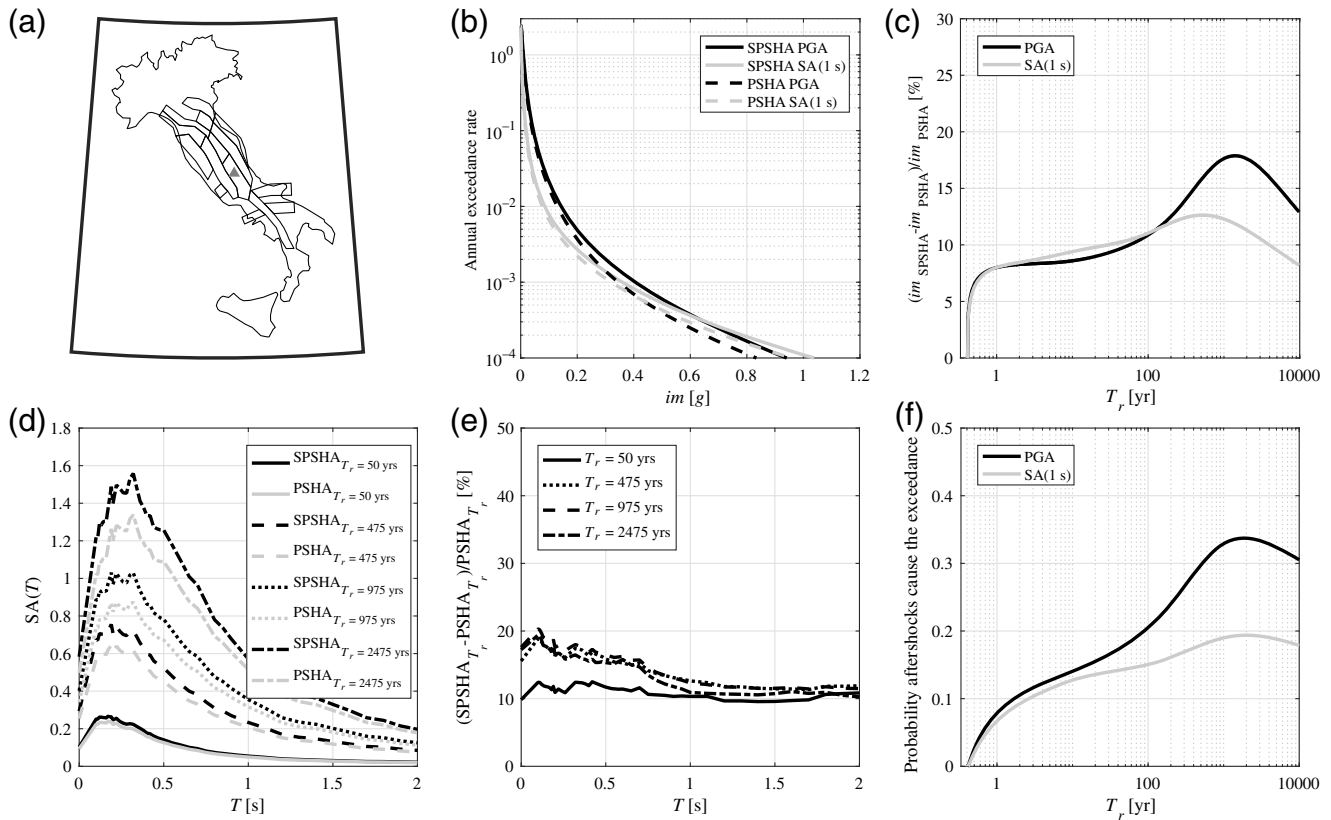


**Figure 6.** Results of hazard analyses for L'Aquila: (a) location of the site and source zones contributing to its hazard; (b) hazard curves for PGA and SA(1 s); (c) hazard increase as a function of the exceedance rate of  $im$ ; (d) uniform hazard spectra (UHS) for 50, 475, 975, and 2475 yrs; (e) hazard increase as a function of the spectral period and for fixed return periods; and (f) aftershock disaggregation for PGA and SA(1 s).

representative of the high (L'Aquila) and low (Milan) hazard according to classical PSHA (see Figs. 2 and 3).

Results for L'Aquila are given in Figure 6. More specifically, Figure 6a shows the site location and the 15 seismogenic zones contributing to the hazard (i.e., within 200 km). The zone in which the site is enclosed is 923, which is one of the three zones from Meletti *et al.* (2008) with the largest maximum magnitude (the others are 929 and 935; see Table 1). In Figure 6b, the hazard curves for PGA (black lines) and SA(1 s) (gray lines) are reported (dashed is PSHA and solid is SPSHA). The range of IM, in which the analyses are performed, is such that the maximum return period is equal to 10,000 yrs. The maximum rate is 2.41, which is the rate of mainshocks occurring within 200 km from the site; that is,

the rate of exceedance when IM tends to zero, see equations (1) and (2). Figure 6c reports the increase of  $im$  between SPSHA and PSHA as a function of the decreasing rate of exceedance (i.e., increasing return period). These differences are nonmonotonic for both PGA and SA(1 s). The maximum increase for PGA is 17.9% and it occurs for a return period of 1350 yrs whereas the maximum increase for SA(1 s), equal to 12.6%, corresponds to a return period of about 530 yrs. The nonmonotonic trend of hazard increase motivates the evidence that the maximum increase for SA(1 s) at a national scale occurs at a 475 yr return period (see Table 2). UHS for the four return periods of 50, 475, 975, and 2475 yrs are reported in Figure 6d. The spectra, indicated as  $PSHA_{T_r}$  and  $SPSHA_{T_r}$ , are computed consider-

**Table 2**  
Nationwide Percentage and Maximum Increase of  $im$  of Sequence-Based Probabilistic Seismic Hazard Analysis (SPSHA) with Respect to PSHA

$T_r$ (yr)	PGA				SA(1 s)			
	50	475	975	2475	50	475	975	2475
Average percentage difference (%)	9.7	10.1	10.3	9.8	10.4	8.7	8.0	7.0
Maximum percentage difference (%)	16.4	22.3	25.6	27.9	16.2	16.7	16.6	14.8
Maximum absolute difference (g)	0.012	0.058	0.084	0.116	0.007	0.035	0.051	0.075

PGA, peak ground acceleration; SA(1 s), spectral accelerations at 1 s natural vibration period;  $T_r$ , return period.

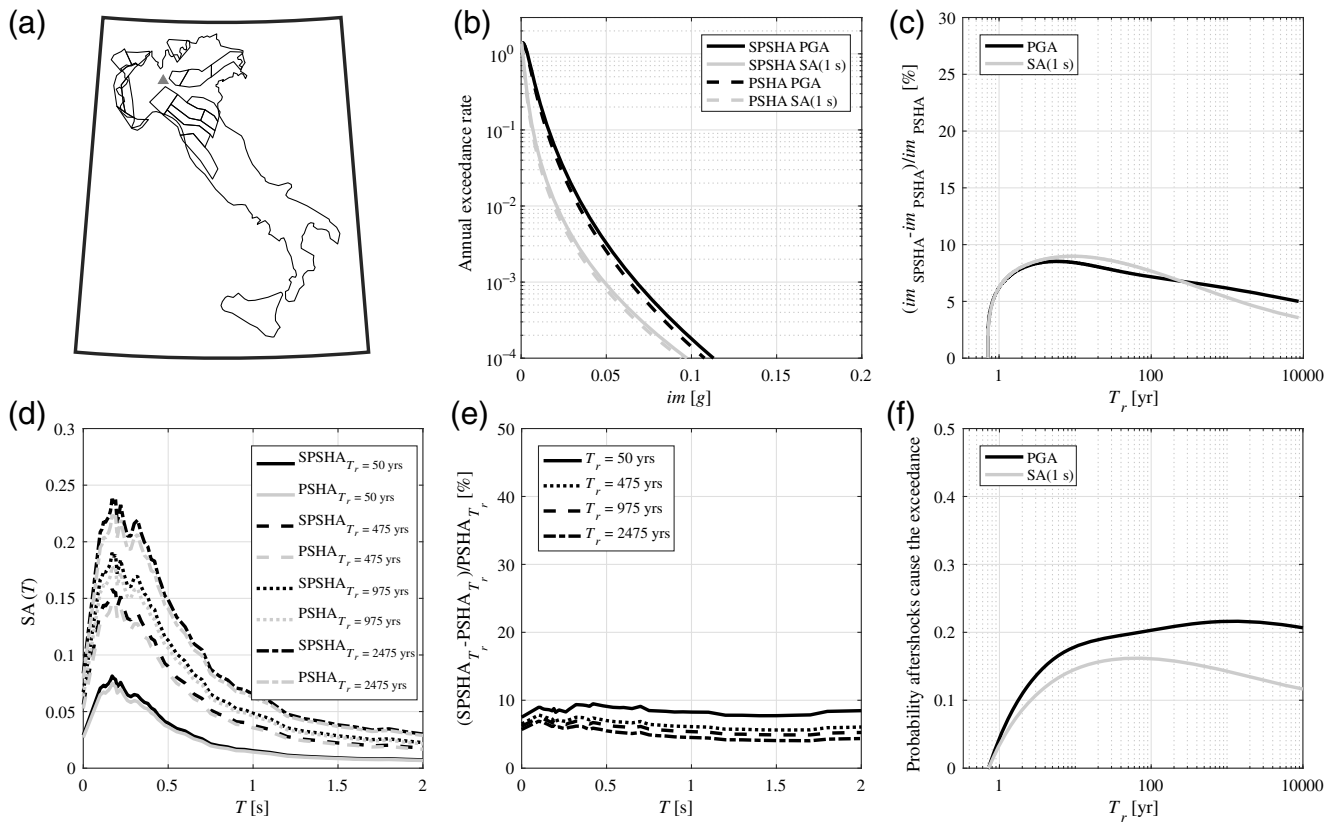


**Figure 7.** Results of hazard analyses for Milan: (a) location of the site and source zones contributing to its hazard; (b) hazard curves for PGA and SA(1 s); (c) hazard increase as a function of the exceeding rate of the  $im$ ; (d) UHS for 50, 475, 975, and 2475 yrs; (e) hazard increase as a function of the spectral period and for fixed return periods; and (f) aftershock disaggregation for PGA and SA(1 s).

ing the 47 natural vibration (spectral) periods  $T$  between 0 and 2 s provided by the adopted GMPE. Increase between SPSHA and PSHA for the selected return periods is reported in Figure 6e as a function of the spectral period. When the return period is 50 yrs, hazard increase is about 10% for all the vibration periods. On the other hand, for return periods of 475, 975, and 2475 yrs, hazard increase is between 15% and 20% for spectral periods lower than 0.7s and between 10% and 15% for spectral periods larger than 0.7s. Finally, aftershock disaggregation is reported in Figure 6f as a function of the increasing return period. As discussed above, SPSHA disaggregation according to equation (4) provides the probability that, once exceedance of  $im$  is observed, it is caused by an aftershock rather than a mainshock; in this sense, it may help in assessing the contribution of aftershock to hazard. Also these curves show a nonmonotonic trend. The probability that exceedance of the IM threshold of interest is caused by aftershocks initially rises with the rising return period. The maximum values of probability from aftershock disaggregation are equal to 0.34 for PGA and 0.19 for SA(1 s), and correspond to  $T_r = 1900$  and 2000 yrs, respectively. For longer return periods, aftershock disaggregation decreases. The difference in disaggregation curves for PGA and for SA(1 s) is such that at the lower return periods the contribution of aftershocks is similar for the two spectral

ordinates, while at the larger return periods it is larger for PGA than SA(1 s). This may provide insight into the trends observed in Figure 6e.

Figure 7 shows the analogous results for Milan. The site is not enclosed in any seismogenic zone and its hazard is affected by the zones reported in Figure 7a. The rates of earthquake occurrence above minimum magnitude (i.e., the value that hazard curves tend toward when IM tends toward zero) is 1.40 and the considered maximum return period is, similarly to the previous case, 10,000 yrs. Hazard curves for PGA and SA(1 s) are reported in Figure 7b while increases are in Figure 7c. In the latter, maximum values are equal to 8.5% and 9.0% for PGA and SA(1 s), respectively. The corresponding return periods are 6 and 10 yrs. Figure 7d shows the UHS for the four return periods. Hazard increase (Fig. 7e) due to SPSHA with respect to PSHA is, for this site, between about 4% and 10% for all the vibration periods and return periods considered here. However, the largest increases are observed for the lower return periods, which is explained by the trend observed in Figure 7c for PGA and SA(1 s). Hazard disaggregation is reported in Figure 7f: maximum probability value for PGA is 0.22 and it corresponds to a return period of 1200 yrs whereas maximum SA(1 s) is 0.16 for an  $im$  threshold with 60 yrs exceedance return period. It should be noted that the maximum values of the probability that an aftershock is

causative for exceedance in Milan are significantly lower with respect to the case of L'Aquila, mainly because the former site is outside any seismic source zone, while the latter is within one of the most seismically relevant, as per Table 1. To more deeply consider how the trends observed at this and the other site depend on an interplay of source–site configuration, the interested reader is referred to Chioccarelli *et al.* (2018).

## Conclusions

SPSHA includes the aftershock's effect in probabilistic seismic hazard assessment. The modified hazard integral relies on the modified Omori law and is probabilistically rigorous in the framework of the considered models. The SPSHA stochastic model was introduced in 2014; herein, it is applied at a national scale using Italy as a case study. The hazard increase due to aftershocks is evaluated considering the same source model lying at the basis of the official seismic hazard of Italy used for structural design. Comparison was carried out in terms of maps of two spectral ordinates with four return periods of exceedance between 50 and 2475 yrs on rock site conditions, as well as full hazard curves and SPSHA disaggregation for two sites differently exposed to seismic hazard according to classical PSHA. Beyond the obvious fact that accounting for the aftershocks' effect increases the hazard in Italy, the analysis allowed pointing out the following issues:

- increase of  $im$  for a given return period can be as high as about 30%; in absolute terms, up to  $0.12g$  for PGA when the return period of the exceedance is 2475 yrs (the site for which the percentage increase is maximum is not the one for which the absolute increase is the largest);
- as expected, the increase due to aftershocks tends to be more significant within or around areas exposed to comparatively higher hazard according to classical PSHA; however, increases are not analogous for different IMs, for example, PGA and SA(1 s), which is consistent with the fact that magnitudes and source-to-site distances contribute differently to hazard of different spectral ordinates;
- disaggregation of sequence-based probabilistic hazard, at least in the considered examples, shows that the contribution of hazard is not monotonic with the increasing return period of exceedance (the specific trend at each site depends on the source–site configuration).

It may be concluded that, notwithstanding the working hypothesis behind this application, which could be refined in more detailed studies, introducing Omori-type aftershock sequences can have a nonnegligible effect on design actions in Italy.

## Data and Resources

All data and resources used in this study are from the listed references, except magnitude rates, which were kindly

provided by Carlo Meletti (Istituto Nazionale di Geofisica e Vulcanologia, Pisa, Italy).

## Acknowledgments

This work was developed within the Rete dei Laboratori Universitari di Ingegneria Sismica (ReLUIIS) 2014–2018 framework program. The authors thank Racquel K. Hagen (Stanford University, California) for having proof-read the article.

## References

- Ambraseys, N. N., K. A. Simpson, and J. J. Bommer (1996). Prediction of horizontal response spectra in Europe, *Earthq. Eng. Struct. Dynam.* **25**, 371–400.
- Beauval, C., S. Hainzl, and F. Scherbaum (2006). Probabilistic seismic hazard estimation in low-seismicity regions considering non-Poissonian seismic occurrence, *Geophys. J. Int.* **164**, 543–550.
- Bommer, J. J., J. Douglas, and F. O. Strasser (2003). Style-of-faulting in ground-motion prediction equations, *Bull. Earthq. Eng.* **1**, 171–203.
- Boyd, O. S. (2012). Including foreshocks and aftershocks in time-independent probabilistic seismic hazard analyses, *Bull. Seismol. Soc. Am.* **102**, 909–917.
- Chioccarelli, E., P. Cito, and I. Iervolino (2018). Disaggregation of sequence-based seismic hazard, *Proc. of the 16th Conf. on Earthquake Engineering, 16ECEE*, Thessaloniki, Greece, 18–21 June 2018.
- Cornell, C. A. (1968). Engineering seismic risk analysis, *Bull. Seismol. Soc. Am.* **58**, 1583–1606.
- Gardner, J. K., and L. Knopoff (1974). Is the sequence of earthquakes in southern California, with aftershocks removed, Poissonian? *Bull. Seismol. Soc. Am.* **64**, no. 5, 1363–1367.
- Gutenberg, B., and C. F. Richter (1944). Frequency of earthquakes in California, *Bull. Seismol. Soc. Am.* **34**, 185–188.
- Iervolino, I., E. Chioccarelli, and P. Cito (2016). REASSESS V1.0: A computationally-efficient software for probabilistic seismic hazard analysis, *Proc. of the VII European Congress on Computational Methods in Applied Sciences and Engineering, ECCOMAS*, Crete Island, Greece, 5–10 June 2016.
- Iervolino, I., E. Chioccarelli, and V. Convertito (2011). Engineering design earthquakes from multimodal hazard disaggregation, *Soil Dynam. Earthq. Eng.* **31**, no. 9, 1212–1231.
- Iervolino, I., M. Giorgio, and B. Polidoro (2014). Sequence-based probabilistic seismic hazard analysis, *Bull. Seismol. Soc. Am.* **104**, 1006–1012.
- Lolli, B., and P. Gasperini (2003). Aftershocks hazard in Italy, Part I: Estimation of time-magnitude distribution model parameters and computation of probabilities of occurrence, *J. Seismol.* **7**, 235–257.
- Marzocchi, W., and M. Taroni (2014). Some thoughts on declustering in probabilistic seismic-hazard analysis, *Bull. Seismol. Soc. Am.* **104**, 1838–1845.
- McGuire, R. K. (2004). *Seismic Hazard and Risk Analysis*, Earthquake Engineering Research Institute, MNO-10, Oakland, California.
- Meletti, C., F. Galadini, G. Valensise, M. Stucchi, R. Basili, S. Barba, G. Vanucci, and E. Boschi (2008). A seismic source zone model for the seismic hazard assessment of the Italian territory, *Tectonophysics* **450**, 85–108.
- Montaldo, V., E. Faccioli, G. Zonno, A. Akinci, and L. Malagnini (2005). Treatment of ground-motion predictive relationships for the reference seismic hazard map of Italy, *J. Seismol.* **9**, 295–316.
- Polidoro, B., I. Iervolino, M. Giorgio, and E. Chioccarelli (2013). Models and issues in history-dependent mainshock hazard, *Proc. of the 11th Conference on Structural Safety and Reliability, ICOSSAR '13*, New York, New York, 16–20 June 2013.
- Reiter, L. (1990). *Earthquake Hazard Analysis: Issues and Insights*, Columbia University Press, New York, New York.
- Stucchi, M., C. Meletti, V. Montaldo, H. Crowley, G. M. Calvi, and E. Boschi (2011). Seismic hazard assessment (2003–2009) for the Italian building code, *Bull. Seismol. Soc. Am.* **101**, 1885–1911.

Utsu, T. (1961). A statistical study on the occurrence of aftershocks, *Geophys. Mag.* **30**, 521–605.

Utsu, T. (1970). Aftershocks and earthquake statistics (1): Some parameters which characterize an aftershock sequence and their interrelations, *J. Faculty Sci., Hokkaido Univ., Ser. 7, Geophys.* **3**, 129–195.

Yeo, G. L., and C. A. Cornell (2009). A probabilistic framework for quantification of aftershock ground-motion hazard in California: Methodology and parametric study, *Earthq. Eng. Struct. Dynam.* **38**, 45–60.

- $IM_A$ : single aftershock IM;
- $IM_{UA}$ : maximum aftershock IM during a sequence.

The sought probability refers to the event that, once exceedance of IM is observed, such exceedance is caused by an aftershock. Such a probability is formulated considering two events: (1) exceedance is observed and could have occurred in the mainshock and/or during the aftershock sequence ( $IM_E > im \cup IM_{UA} > im$ ); and (2) exceedance is observed in the aftershock sequence and it is not observed in the mainshock ( $IM_E \leq im \cap IM_{UA} > im$ ). Consequently, the sought probability is  $P[IM_E \leq im \cap IM_{UA} > im | IM_E > im \cup IM_{UA} > im]$ , which can be written as:

## Appendix

This appendix provides the derivation of aftershock disaggregation given in equation (4). The symbols used in the

$$P[IM_E \leq im \cap IM_{UA} > im | IM_E > im \cup IM_{UA} > im] = \frac{P[IM_E > im \cup IM_{UA} > im | IM_E \leq im \cap IM_{UA} > im] \cdot P[IM_E \leq im \cap IM_{UA} > im]}{P[IM_E > im \cup IM_{UA} > im]} = \frac{P[IM_E \leq im \cap IM_{UA} > im]}{P[IM_E > im \cup IM_{UA} > im]}, \quad (A1)$$

derivation, some of which have been given already in the text, are as follows:

- $v_E$ : mainshock (and sequence) occurrence rate;
- $M_E \in (m_{E,\min}, m_{E,\max})$ : mainshock magnitude;
- $M_A \in (m_{\min}, x)$ : aftershock magnitude;
- $R_E \in (r_{E,\min}, r_{E,\max})$ : mainshock source-to-site distance;
- $R_A \in (r_{A,\min}, r_{A,\max})$ : aftershock source-to-site distance;

in which it is easy to recognize that  $P[IM_E > im \cup IM_{UA} > im | IM_E \leq im \cap IM_{UA} > im] = 1$ . This is because, given that exceedance has been observed during the aftershock sequence, it is certain that exceedance has been observed; that is, the latter event is included in the former ( $IM_E > im \cup IM_{UA} > im \supseteq IM_E \leq im \cap IM_{UA} > im$ ). Now, applying the total probability theorem to the numerator of equation (A1) gives:

$$\frac{P[IM_E \leq im \cap IM_{UA} > im]}{P[IM_E > im \cup IM_{UA} > im]} = \frac{\iint_{M_E, R_E} P[IM_E \leq im \cap IM_{UA} > im | x, y] \cdot f_{M_E, R_E}(x, y) \cdot dx \cdot dy}{P[IM_E > im \cup IM_{UA} > im]} = \frac{\iint_{M_E, R_E} P[IM_E \leq im | x, y] \cdot P[IM_{UA} > im | x, y] \cdot f_{M_E, R_E}(x, y) \cdot dx \cdot dy}{P[IM_E > im \cup IM_{UA} > im]}. \quad (A2)$$

- $E[N_{A|x}(0, \Delta T_A)]$ : mean number of aftershocks in a sequence of duration  $\Delta T_A$  triggered by a mainshock of  $M_E = x$ ;
- $E[N_{A,im|x}(0, \Delta T_A)]$ : mean number of aftershocks exceeding the  $im$  threshold in a sequence of duration  $\Delta T_A$  triggered mainshock of  $M_E = x$ ;
- $\lambda_{im}$ : rate of exceedance of  $im$  according to sequence-based probabilistic seismic hazard analysis (SPSHA);
- $IM_E$ : mainshock intensity measure (IM);

In this latter equation, it is considered that the IMs of mainshocks and aftershocks are conditionally independent given the mainshock features (Yeo and Cornell, 2009).

It can now be recognized that the probability that exceedance of IM is observed during the aftershock sequence is given by the following equation, which follows the non-homogeneous Poisson processes (NHPP) assumption of aftershock PSHA (APSHA; see Iervolino *et al.*, 2014):

$$P[IM_{UA} > im | x, y] = 1 - e^{-E[N_{A,im|x}(0, \Delta T_A)]} = 1 - e^{-E[N_{A|x}(0, \Delta T_A)] \cdot \iint_{M_A, R_A} P[IM_A > im | w, z] \cdot f_{M_A, R_A | M_E, R_E}(w, z | x, y) \cdot dw \cdot dz}. \quad (A3)$$

At this point, replacing equation (A3) in equation (A2), and multiplying numerator and denominator by  $\nu_E$ , provides the sought result:

$$P[\text{IM}_E \leq im \cap \text{IM}_{\cup A} > im | \text{IM}_E > im \cup \text{IM}_{\cup A} > im] \\ = \frac{\nu_E}{\lambda_{im}} \cdot \iint_{M_E, R_E} P[\text{IM}_E \leq im | x, y] \cdot \left( 1 - e^{-E[N_A | x, (0, \Delta T_A)]} \cdot \iint_{M_A, R_A} P[\text{IM}_A > im | w, z] \cdot f_{M_A, R_A | M_E, R_E}(w, z | x, y) \cdot dw \cdot dz \right) \cdot f_{M_E, R_E}(x, y) \cdot dx \cdot dy. \quad (\text{A4})$$

The equation takes advantage of  $\nu_E \cdot P[\text{IM}_E > im \cup \text{IM}_{\cup A} > im] = \lambda_{im}$ . In fact, the rate of exceedance of  $im$  in SPSHA is the rate of occurrence of seismic sequences times the probability that a sequence causes at least one exceedance of  $im$ .

Dipartimento di Strutture per l'Ingegneria e l'Architettura  
Università degli Studi di Napoli Federico II  
via Claudio 21  
80125 Naples, Italy  
iunio.iervolino@unina.it  
(I.I.)

Università Telematica Pegaso  
Piazza Trieste e Trento 48  
80132 Naples, Italy  
eugenio.chioccarelli@unipegaso.it  
(E.C.)

Dipartimento di Ingegneria  
Università degli Studi della Campania Luigi Vanvitelli  
via Roma 29  
80131 Aversa (CE), Italy  
massimiliano.giorgio@unicampania.it  
(M.G.)

Manuscript received 10 November 2017;  
Published Online 10 July 2018